# Towards real-time non contact spatial resolved oxygenation monitoring using a multi spectral filter array camera in various light conditions

Jacob R. Bauer, Karlijn van Beekum, John Klaessens, Herke Jan Noordmans, Christa Boer, et al.

Jacob R. Bauer, Karlijn van Beekum, John Klaessens, Herke Jan Noordmans, Christa Boer, Jon Y. Hardeberg, Rudolf M. Verdaasdonk, "Towards real-time non contact spatial resolved oxygenation monitoring using a multi spectral filter array camera in various light conditions," Proc. SPIE 10489, Optical Biopsy XVI: Toward Real-Time Spectroscopic Imaging and Diagnosis, 104890O (19 February 2018); doi: 10.1117/12.2288432

SPIE.

Event: SPIE BiOS, 2018, San Francisco, California, United States

# Towards real-time non contact spatial resolved oxygenation monitoring using a multi spectral filter array camera in various light conditions

Jacob R. Bauer[a], Karlijn van Beekum[b], John Klaessens[b], Herke Jan Noordmans[c], Christa Boer[b], Jon Y. Hardeberg[a], and Rudolf M. Verdaasdonk[b]

[a]Norwegian University of Science and Technology, The Norwegian Colour and Visual Computing Laboratory, Gjøvik, Norway
[b]VU University Medical Center, Dept. of Physics & Medical Technology, Amsterdam, Netherlands
[c]University Medical Center Utrecht, Dept. of Medical Technology and Clinical Physics, Utrecht, Netherlands

## ABSTRACT

Non contact spatial resolved oxygenation measurements remain an open challenge in the biomedical field and non contact patient monitoring. Although point measurements are the clinical standard till this day, regional differences in the oxygenation will improve the quality and safety of care. Recent developments in spectral imaging resulted in spectral filter array cameras (SFA). These provide the means to acquire spatial spectral videos in real-time and allow a spatial approach to spectroscopy. In this study, the performance of a 25 channel near infrared SFA camera was studied to obtain spatial oxygenation maps of hands during an occlusion of the left upper arm in 7 healthy volunteers. For comparison a clinical oxygenation monitoring system, INVOS, was used as a reference. In case of the NIRS SFA camera, oxygenation curves were derived from 2-3 wavelength bands with a custom made fast analysis software using a basic algorithm. Dynamic oxygenation changes were determined with the NIR SFA camera and INVOS system at different regional locations of the occluded versus non-occluded hands and showed to be in good agreement. To increase the signal to noise ratio, algorithm and image acquisition were optimised. The measurement were robust to different illumination conditions with NIR light sources. This study shows that imaging of relative oxygenation changes over larger body areas is potentially possible in real time.

**Keywords:** spectral filter array camera, non- contact monitoring, near infrared, oxygenation, skin assessment, optical diagnosis,

## 1. INTRODUCTION

Light reflected from skin undergoes interactions within the tissue and the resulting reflected spectrum carries useful information, like chromophore concentrations,[1] blood perfusion[2] and information about the oxygenation of skin tissue.[3] Oxygenation is a useful health metric indicating nutrition supply and homeostasis of tissue. The oxygenation information can be used to indicate cancerous regions,[4] give insides into wound healing processes of chronic wounds, and can be utilized as a first care measurement indicating the severity of burn-wounds.[5] Next to visual assessment of the skin, so called diffuse reflectance spectroscopy is utilized in the clinics. These are spectral point measurements and are used for measuring oxygen concentration or the concentration of other chromophores present in superficial skin tissue. Diffuse reflectance spectroscopy is often based on optical fibers and a defined optical setup. Most commonly one fiber is used to deliver the light to the tissue surface and one or more fibers are used to sense the diffuse reflectance from the tissue and measures spectra through a diffraction grating. Through Monte Carlo modeling or diffusion theory chromophore concentrations in the skin

Further author information: (Send correspondence to J.R.Bauer)
J.R.Bauer: E-mail: jacob.bauer@ntnu.no, Telephone: 0049 173 421 3461

Optical Biopsy XVI: Toward Real-Time Spectroscopic Imaging and Diagnosis, edited by Robert R. Alfano, Stavros G. Demos
Proc. of SPIE Vol. 10489, 104890O · © 2018 SPIE · CCC code: 1605-7422/18/$18 · doi: 10.1117/12.2288432

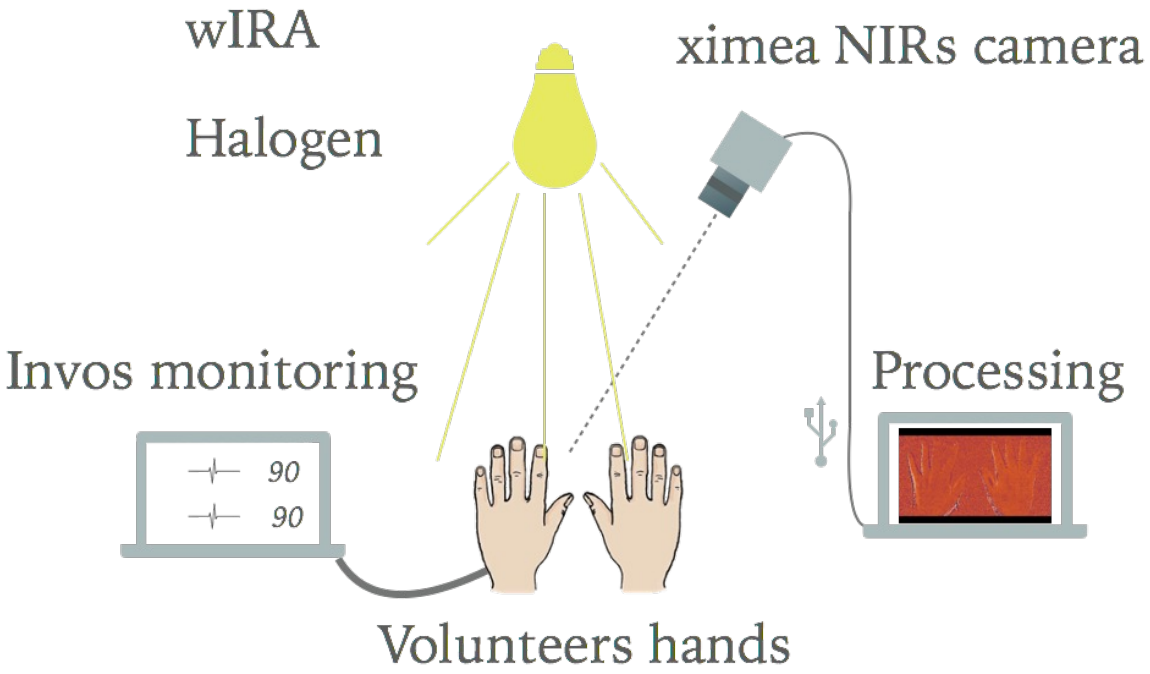


Figure 1. experimental setup, parallel measurement of spectral reflectance with the NIR SFA camera and the clinically approved INVOS system

can be derived. Diffuse reflectance spectroscopy is limited to point measurements and therefore measure the oxygen saturation in a small area. Since the oxygenation or oxygen concentration differs greatly throughout the tissue a spatially resolved measurement could be beneficial. It has been shown that spectral imaging using various different techniques could be applied.[6–8] Most commonly spectral imaging techniques, like spectral filter wheels, liquid crystal filter cameras resolve the spectral dimension through time variant sampling. Spectral filter array cameras on the other hand are a new type of spectral imaging devices with the ability to acquire a spectral cube in a single shot within milliseconds preventing motion artifacts due to time difference between spectral channels as with common spectral imaging techniques. Since blood perfusion and oxygen distribution is a dynamic process, information is lost if the spectral sampling is performed over time. In this study, capabilities of a commercially available spectral filter array (SFA) near infrared (NIR) camera manufactured by XIMEA (XiSpec MQ022HG-IM-SM5X5-NIR) with an IMEC sensor as a spatially resolved oxygenation measurement were studied. We hereby focus on the postprocessing steps necessary in order to derive oxygenation readings and compare with a clinical system (INVOS Somanetics 5100 C of Covidien) as local point oxygenation measurement tool.

## 2. METHODS

As proof of concept measurements were conducted in 11 healthy volunteers. The volunteers placed their hands on the measurement table with a distance of around 1cm between their hands. The experimental setup is shown in Figure 1. The so called upper arm occlusion protocol was used, where pressure was applied to the left upper arm using an inflatable cuff. Through the cuff the blood flow into the left hand was occluded, while the right hand blood circulation is unaltered. The hands of the volunteer were measured continuously both with the multispectral SFA camera and the INVOS spectroscopy device. First a baseline measurement was performed for 2 minutes without applying any pressure. Followed by 3 minutes of measuring the hands with the cuff inflated and occlusion applied for 3 minutes. The pressure applied was around 160mmHg and a marker was added to the imaged scene as soon as the occlusion was applied. After the occlusion phase, another 5 minutes was acquired of the re-perfusion phase. All volunteers were measured twice with 1 day in-between in order to allow inter measurement comparison.

Table 1. Settings for the XIMEA camera for the measurements

| | Halogen light source |
|---|---|
| Filter range | 600  875 nm |
| Aperture | 1.65 |
| RAW | 16 |
| Exposure | 19 ms |
| Gain | 0.00 dB |
| FPs | 1.00 |
| Limit bandwidth | 2843 Mbit/s |
| Manual WB (R : G : B) | 1.00 : 1.00 : 1.00 |

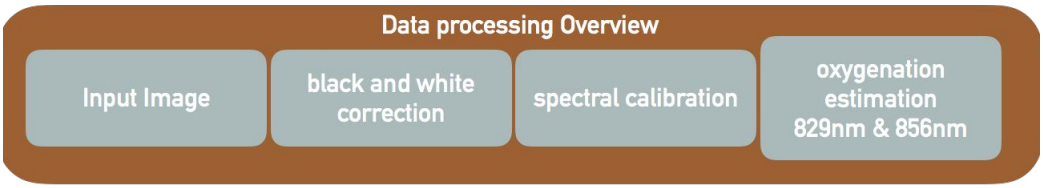


Figure 2. Overview of the dataprocessing for the NIR SFA data

## 2.1 Multispectral Imaging

The multispectral measurements included in this research are performed using the XIMEA (MQ022HG-IM-SM5X5-NIR camera) and the Xicam (acquisition) tool by XIMEA. In addition, a custom build software program 'Multispec' (developed by Herke Jan Noordmans from the UMC Utrecht, The Netherlands) was used for the data processing of the 25 narrow band snap shot spectral images. The spectral sensitivity is in the NIR range between 600nm-875nm. A 'dark' image was obtained for background noise correction.

In addition, a flat field correction was performed using a uniform grey surface to account for an in-homogenous illumination of the scene and to account for the unique spectral power distribution of the light source.

A grey correction target was used in order to allow for the same exposure time, aperture and frames per second seconds compared to the test measurements of the hand. Therefore the final image was given as:

$$I_n(x,y) = \frac{I_{Sn}(x,y) - I_{Dn}(x,y)}{I_{Wn}(x,y - I_{Dn}(x,y)} \tag{1}$$

The final image was given by dividing the sample image minus the dark current image divided by the grey sheet image minus the dark image. Due to considerable overlap of the different spectral channels, a spectral correction was necessary and reduced the number of effective channels to 10. The correction is performed via a matrix operation with correction values reported by the camera manufacturer, which are based on the specific spectral sensitivities of the camera. Figure 2 shows the final data processing steps in order to arrive at the oxygenation estimations based on the NIR SFA camera. The selected camera parameters for acquisition can be found in Table 1. A sequence of 1 frame per second during 15 minutes was acquired.

### 2.1.1 Light source

The Measurements were performed with a halogen light source which spectra is shown in Figure 3. It is a continuous lightsource, which is commercially available. This was important to ensure a save use in the clinic and at the same time guarantee enough light intensity in the near infrared. For the setup in order to avoid specular reflections the lightsource was used in a 45° angle towards the imaging equipment.

## 2.2 Reference measurements

As references for the oxygenation, the INVOS Semantics 5100 C was used with a contact sensor attached to the palms of both hands. The sensors were attached tightly to the palm of the hand to ensure consistent readings with the INVOS system. Both measurements were performed at the same time and continuous oxygenation measurements were acquired. In contrast to the multispectral measurements, the INVOS system performed a

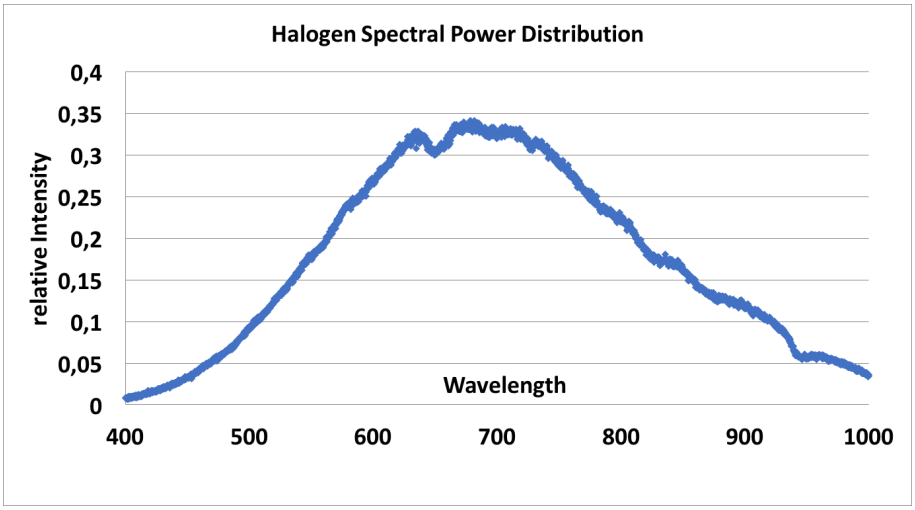


Figure 3. Halogen light source spectral power distribution measurement with Thorlabs

measurement every 5-6 seconds. In order to align both measurements the moment of occlusion was marked in the the INVOS system, simultaneously a marker was added to the imaged scene. This allows to mark the timepoint of occlusion and that of the release of the pressure inflatable cuff up to the reaction times of the researcher conducting the measurements.

### 2.3 Data analysis for Oxygenation estimation

The SFA camera used in this research provides a spatially resolved measure of 25 different wavelengths reflected from the image scene. This information has to be utilized in order to estimate the oxygenation of the tissue in different regions or spatially resolved per pixel. For this research, oxygenation estimation algorithms where applied, which can potentially be performed in real time. The modified Beer-Lambert method was used which has been previously reported as the $\Delta t$ method in some publications[9–11] The basis for this method lies in the modified Beer-Lambert and considers absorption and scattering the main reasons for the attenuation of light in skin. This method assumes a change of absorption over time due to the concentration of chromophores present in the skin: in particular, the differences in oxy-, and deoxy- hemoglobin concentration present in the skin. Part of the total absorption of skin is hereby considered to be constant, due to other unchanged chromophores present in the skin. oxy- and deoxy- hemoglobin concentration are considered to change over time during the measurement and are the property of investigation. The Optical density or absorption can be defined as:

$$OD = -log_{10}(\frac{I}{I_0}) = \sum_n \varepsilon_n * c_n * d, \tag{2}$$

where OD stands for optical density $I_0$ is the emitted light intensity, and $I$ is the intensity of the received light, $\varepsilon$ describes the molar extinction coefficient for $n$ different chromophores, $c$ describes the concentration of the chromophore $n$ and $d$ describes the path-length for the light. Since scattering increases the path-length of light travelling through the tissue the modified Beer-Lambert law[12] can be used to describe this with:

$$\overline{A(\lambda)} = \overline{\varepsilon(\lambda)} * \overline{c(t)} * \overline{D_{PF}(\lambda)} * d + \overline{G(\lambda)} + \overline{H(t)}, \tag{3}$$

where $\overline{A(\lambda)}$ is the absorbance [-], $\overline{\varepsilon(\lambda)}$ describes the molar extinction coefficient $[mM^{-1}cm^{-1}]$, $\overline{c(t)}$ is the concentration of a specific chromophore$[mM]$, $\overline{D_{PF}(\lambda)}$ differential path length factor corrects the geometrical source-detector distance to the mean optical path in the tissue, $d$ the source detector distance $[cm]$, and $\overline{G(\lambda)}$ and $\overline{H(t)}$ are both oxygen independant loss factors accounting for scattering, absorption and geometry losses where $\overline{H(t)}$ is time dependant and $\overline{G(\lambda)}$ is wavelength dependant.

This can be rewritten in matrix form and with i.e. 3 specific wavelength to:

$$\begin{bmatrix} A(\lambda_1,t) \\ A(\lambda_2,t) \\ A(\lambda_3,t) \end{bmatrix} = \begin{bmatrix} \varepsilon_{O_2Hb}(\lambda_1)D_{PF}(\lambda_1) & \varepsilon_{HHb}(\lambda_1)D_{PF}(\lambda_1) \\ \varepsilon_{O_2Hb}(\lambda_2)D_{PF}(\lambda_2) & \varepsilon_{HHb}(\lambda_2)D_{PF}(\lambda_2) \\ \varepsilon_{O_2Hb}(\lambda_3)D_{PF}(\lambda_3) & \varepsilon_{HHb}(\lambda_3)D_{PF}(\lambda_3) \end{bmatrix} * \begin{bmatrix} c_{O_2Hb}(t) \\ c_{HHb}(t) \end{bmatrix} d + \begin{bmatrix} G(\lambda_1) \\ G(\lambda_2) \\ G(\lambda_3) \end{bmatrix} + \begin{bmatrix} H(t) \\ H(t) \\ H(t) \end{bmatrix}$$

Under the assumption that the $H$ term is zero or constant in time and the $G$ term also stays constant during the measurement. Then the differences in concentration in a time interval $\Delta t$ relative to a stable starting point can be calculated. A known $\overline{DPF(\lambda)}$ values from literature for the interrogated tissue have been used to simplify the equation to determine the concentration of a chromophore to:

$$\Delta_t \overline{c} = \frac{\overline{\varepsilon}\,\overline{D_{PF}}^{-1}\Delta_t \overline{A}}{d} \tag{4}$$

For this setup, the use of two different wavelengths (826 and 859nm) proved to be best for the calculation of the oxy-,deoxy- concentration present in the tissue. It allowed to relate changes in reflected light intensity to changes in oxy and deoxy hemoglobin concentration. Consequently, this technique was used to estimate oxygen concentration from our spectral image cubes. This was done in specifically chosen regions of interest which will be described further in the next section.

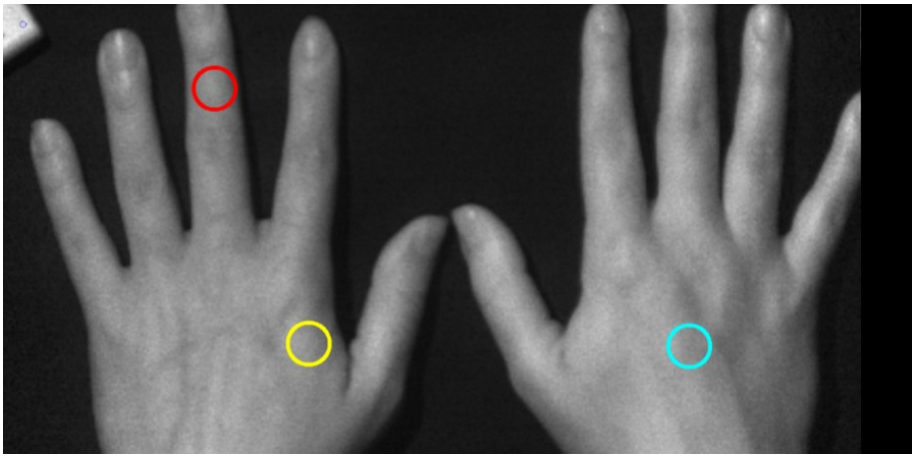

Figure 4. Circles indicate areas of interrogation an average was taken from these pixel areas and the average oxygenation of these areas was plotted over time

## 3. RESULTS

From the images, a region of interest was defined for the estimation of oxygenation in the hands. Figure 4 illustrates these different regions of interest. An average oxygenation concentration was calculated for each region. These areas have been chosen as close to the measurement location of the INVOS system, far away from the measurement location of the INVOS system and it has also been reported that the finger tips show stronger desaturations and lastly one of the regions of interest in the hand without any occlusion was chosen in order to verify the oxygenation behaviour in the unaltered hand.

Figure 5 shows a representative result of one volunteer of estimated oxygen concentration using the halogen light source. In grey is the relative reflected intensity of our marker plotted, which was included into the scene to indicate the occlusion and cuff release. Oxygenation is represented by the blue line and deoxygenation with the orange line. Both follow the expected curves and show good agreement with previously reported occlusion behaviour.[13]

Figure 6 shows that the agreement between INVOS system and estimated oxygenations from the NIR system are close during deoxygenation, reperfusion and "back to baseline". This measurement was chosen as representative for the entire dataset of 11 healthy volunteers. Among all measurements the same trend when compared to

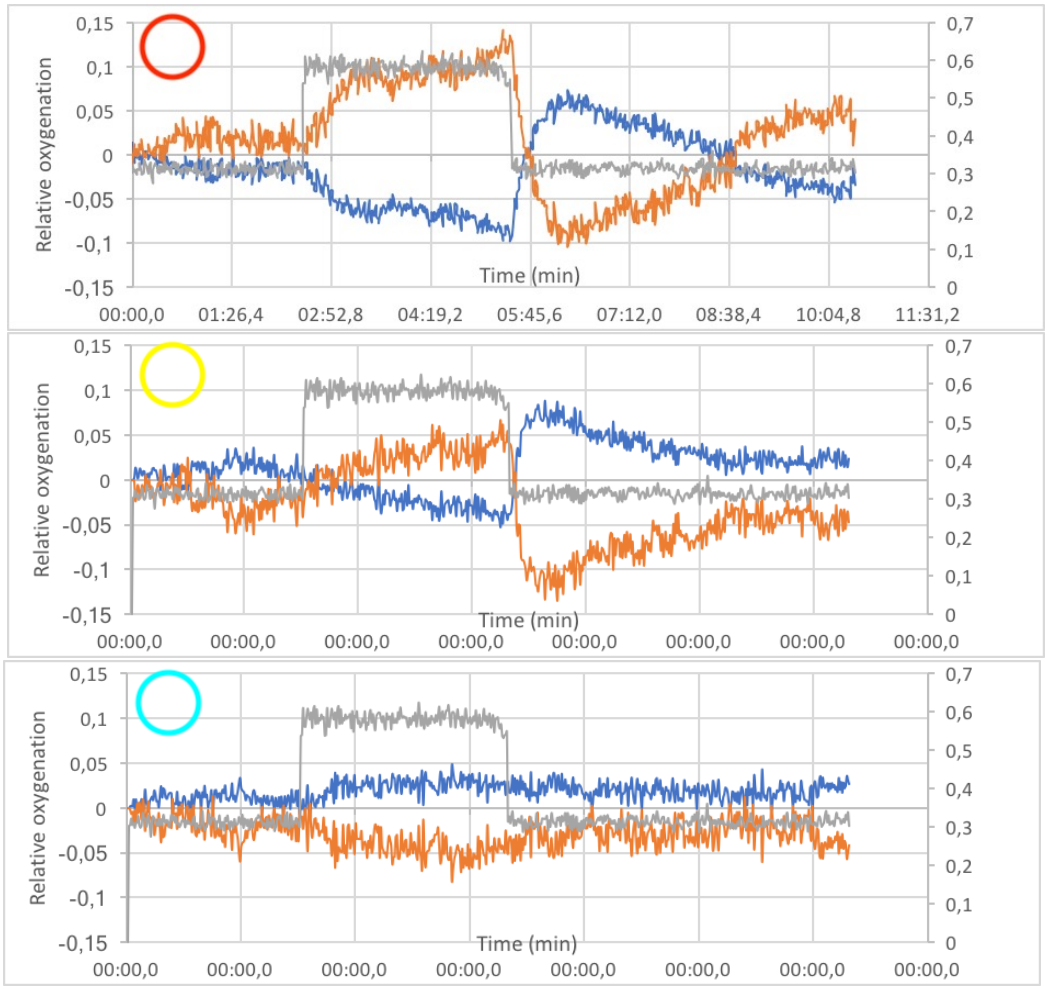


Figure 5. The first graph is a plot of the average estimated oxygen concentration from the finger marked with the red circle in Figure 4. Secondly is the averaged estimated oxygen concentration from the yellow circle back side of the palm and closest to the INVOS measurements. Third plot indicates the reference measurement on the un-occluded hand average area is the cyan circle.

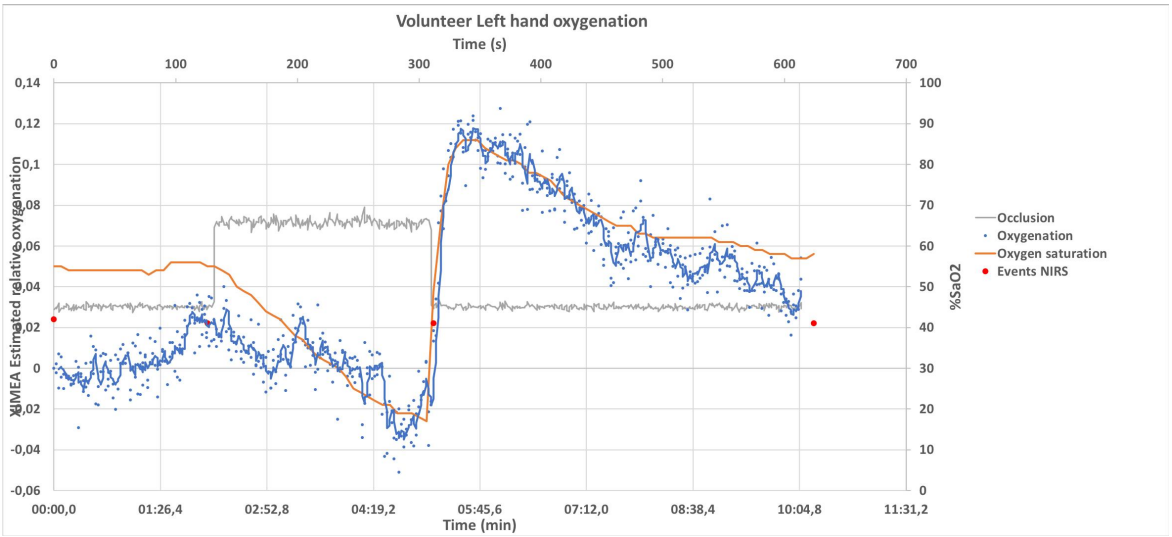


Figure 6. Plot of INVOS oxygenation results (orange solid line) compared to NIR SFA imaging system results (blue line). The results from the NIR SFA imaging system are plotted with a moving average of 4 values represented by the solid line.

the INVOS system was observed with some measurement showing better agreement between the two measurement system then others. A second lightsource was also tested and showed the same trends, but in some patient that second halogen lamp interfered with the ground truth measurements of the INVOS system and therefore is not reported here. In the next section the obtained results and limitations will be discussed.

## 4. DISCUSSION

The goal of this study was to show the potential of the NIR SFA camera as a real time spatial oxygenation measurement tool. Results obtained are promising in regards to the expected oxygenation behaviour in healthy volunteers. In order to apply these techniques in a less controlled clinical setup with unwell patients the method of measurement has to be further improved.

Even though the relative oxygenation curve during the occlusion followed the trends as measured with our reference, the estimation does not provide absolute measurements. Therefore, the curves were aligned regarding the maximum oxygenation present in both signals, since the value range of the oxygen estimations is an arbitrary scale and only shows dynamic and relative changes over time. The oxygenation estimation should be calibrated in order to provide full absolute oxygenation values in a spatially resolved manner. Agreement between these two curves, especially in the regions of "reperfusion" and "back to baseline" is of clinical importance, since they contain information about the arterial health of a patient. The alignment of the curves is arbitrary and could have also be done at the baseline level in the beginning of the measurement. But especially the regions at the start of occlusion and during occlusion and after occlusion are important for clinical use of this data. The general trends especially in these areas can be considered similar. Figure 7 shows the areas which are especially interesting for clinical readings of these occlusion measurements. This indicates that both measurement systems sensed a similar underlying change in oxygenation of the blood present over time. Another factor which has to be taken into account for differences measured between the INVOS system and the NIR SFA camera system is the location of measurement. The increased amount of melanin on the back of the hand can negatively influence the measurements. Due to the fact that we were measuring with the NIR SFA camera the higher absorption of superficial melanin should be minimal. The underlying vessel structures on the other hand can also influence the measurement results. Different locations have shown to be perfused differently, which makes the direct comparison challenging. In the future a direct comparison between the NIR SFA camera and the VIS SFA camera (also distributed by XIMEA) could be done in order to further investigate the difference of sensing superficial oxygenation and deeper blood delivery.

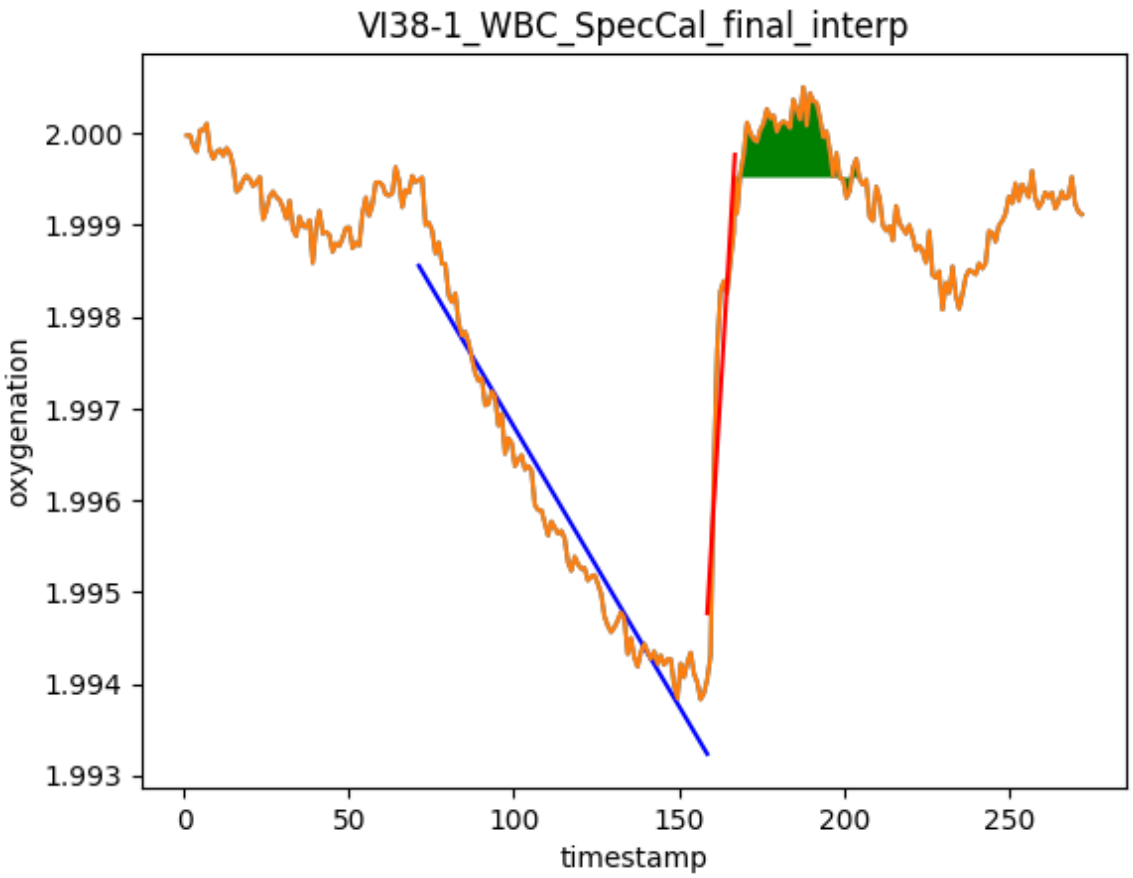


Figure 7. especially the area under the curve, the desaturatuion slope and the resaturation slope (in this figure linear interpolations in specific areas of the oxygenation curve) are of clinical value. In a planned publication we will discuss these further and show the results obtained with the visual range camera

Furthermore, special attention should be taken for the spectral correction and the influence of the method chosen should be further studied this will be part of a future publication focussing on the effect of the spectral correction on the final results. A more robust oxygenation estimation could be performed and the final implementation in real time should be evaluated. Adjustment to guarantee full real time processing should be straight forward with the chosen approach. Furthermore, as shown in Figure 7 a numerical comparison between these marked key features of the two oxygenation results is planned in another publication. These key features of the oxygenation curves provide useful information about the arterial health. This study has limitations including among others the selection of volunteers. The sample size and diversity among the volunteers measured should be improved in order to show robustness against different skin types and other intra volunteer differences. Furthermore, all the volunteers were healthy and patients in care could affect the measurements outcome, due to lower blood pressure. Robustness to these special conditions has to be shown for a clinical application of these methods. Oxygenation estimation could be further improved with additional wavelength to reduce noise and a real time implementation should be feasible. Regardless of the shortcomings mentioned using NIR SFA imaging for spatially resolved oxygenation measurement shows potential for clinical applications.

## 5. CONCLUSION

This research focussed on a method to estimate oxygenation of in vivo tissue using a near infrared spatial filter array camera with low computationally demands. The proposed method shows good agreement with expectations according to the occlusion protocols and agreement with our reference INVOS measurement system especially in

clinically relavent aspects of the oxygenation curves. It can be easily adapted to be performed in real time and provides a relative spatial oxygenation map. In order to ensure feasibility for a clinical setup several improvements for the approach are discussed in the previous section.

## Acknowledgment

This research has been supported by the Research Council of Norway through project no. 247689 IQ-MED: Image Quality enhancement in MEDical diagnosis, monitoring and treatment.

## REFERENCES

[1] MacKinnon, N., Vasefi, F., Gussakovsky, E., Bearman, G., Chave, R., and Farkas, D. L., "In vivo skin chromophore mapping using a multimode imaging dermoscope (SkinSpec)," *SPIE BiOS* **8587**, 85870U–85870U–13 (Feb. 2013).

[2] Randeberg, L. L., Eivind L. P. Larsen, and Svaasand, L. O., "Hyperspectral imaging of blood perfusion and chromophore distribution in skin," *Proc. SPIE BiOS: Biomedical Optics* **7161**, 71610C–71610C–12, International Society for Optics and Photonics (Feb. 2009).

[3] Huang, J., *Multispectral imaging of skin oxygenation*, PhD thesis, The Ohio State University (2013).

[4] Lu, G. and Fei, B., "Medical hyperspectral imaging: a review," *Journal of Biomedical Optics* **19**, 010901–010924 (Jan. 2014).

[5] Sowa, M. G., Leonardi, L., Payette, J. R., Cross, K. M., Gomez, M., and Fish, J., "Classification of burn injuries using near-infrared spectroscopy," *Journal of Biomedical Optics* **11**, 11 – 11 – 6 (2006).

[6] Spigulis, J., Rubins, U., Kviesis-Kipge, E., and Rubenis, O., "SkImager: a concept device for in-vivoskin assessment by multimodal imaging," *Proceedings of the Estonian Academy of Sciences* **63**(3), 301–308 (2014).

[7] Ferguson-Pell, M. and Hagisawa, S., "An empirical technique to compensate for melanin when monitoring skin microcirculation using reflectance spectrophotometry," *Medical Engineering & Physics* **17**(2), 104–110 (1995).

[8] Gioux, S., Mazhar, A., Lee, B. T., Lin, S. J., Tobias, A. M., Cuccia, D. J., Stockdale, A., Oketokoun, R., Ashitate, Y., Kelly, E., Weinmann, M., Durr, N. J., Moffitt, L. A., Durkin, A. J., Tromberg, B. J., and Frangioni, J. V., "First-in-human pilot study of a spatial frequency domain oxygenation imaging system.," *Journal of Biomedical Optics* **16**, 086015–086015–10 (Aug. 2011).

[9] Klaessens, J. H. G. M., Noordmans, H. J., de Roode, R., and Verdaasdonk, R. M., "Non-invasive skin oxygenation imaging using a multi-spectral imaging system, Effectiveness of different concentration algorithms applied on human skin," in [*World Congress on Medical Physics and Biomedical Engineering, September 7 - 12, 2009, Munich, Germany*], 725–728, Springer Berlin Heidelberg, Berlin, Heidelberg (2009).

[10] Klaessens, J. H. G. M., Landman, M., de Roode, R., Noordmans, H. J., and Verdaasdonk, R. M., "Thermographic and oxygenation imaging system for non-contact skin measurements to determine the effects of regional block anesthesia," *Proc.SPIE* **7548**, 7548 – 7548 – 11 (2010).

[11] Klaessens, J. H. G. M., De Roode, R., Verdaasdonk, R. M., and Noordmans, H. J., "Hyperspectral imaging system for imaging o2hb and hhb concentration changes in tissue for various clinical applications," *Proc.SPIE* **7890**, 7890 – 7890 – 10 (2011).

[12] Delpy, D. T., Cope, M., van der Zee, P., Arridge, S., Wray, S., and Wyatt, J., "Estimation of optical pathlength through tissue from direct time of flight measurement," *Physics in Medicine Biology* **33**(12), 1433 (1988).

[13] Nishidate, I., Maeda, T., Niizeki, K., and Aizu, Y., "Estimation of Melanin and Hemoglobin Using Spectral Reflectance Images Reconstructed from a Digital RGB Image by the Wiener Estimation Method," *Sensors* **13**, 7902–7915 (June 2013).